

Bias-Conflict Sample Synthesis and Adversarial Removal Debias Strategy for Temporal Sentence Grounding in Video

Zhaobo Qi¹, Yibo Yuan¹, Xiaowen Ruan¹, Shuhui Wang²,
Weigang Zhang^{1*}, Qingming Huang^{2, 3*}

¹Harbin Institute of Technology, Weihai, China

²Key Lab of Intell. Info. Process., Inst. of Comput. Tech., CAS, Beijing, China

³University of Chinese Academy of Sciences, Beijing, China

qizb@hit.edu.cn, {yuanyibo21,22s130489}@stu.hit.edu.cn, wangshuhui@ict.ac.cn,
wgzhang@hit.edu.cn, qmhuang@ucas.ac.cn

Abstract

Temporal Sentence Grounding in Video (TSGV) is troubled by dataset bias issue, which is caused by the uneven temporal distribution of the target moments for samples with similar semantic components in input videos or query texts. Existing methods resort to utilizing prior knowledge about bias to artificially break this uneven distribution, which only removes a limited amount of significant language biases. In this work, we propose the bias-conflict sample synthesis and adversarial removal debias strategy (BSSARD), which dynamically generates bias-conflict samples by explicitly leveraging potentially spurious correlations between single-modality features and the temporal position of the target moments. Through adversarial training, its bias generators continuously introduce biases and generate bias-conflict samples to deceive its grounding model. Meanwhile, the grounding model continuously eliminates the introduced biases, which requires it to model multi-modality alignment information. BSSARD will cover most kinds of coupling relationships and disrupt language and visual biases simultaneously. Extensive experiments on Charades-CD and ActivityNet-CD demonstrate the promising debiasing capability of BSSARD. Source codes are available at <https://github.com/qzhb/BSSARD>.

Introduction

Temporal sentence grounding in video (TSGV) aims to locate the target video clip corresponding to the query sentence, which plays a vital role in fields such as video creation and video monitoring. With the help of deep learning, TSGV has achieved promising performance (Zhang et al. 2020b; Ghosh et al. 2019; Zhang et al. 2020a; Yuan et al. 2019; Zheng et al. 2023a; Wang et al. 2023). However, recent studies (Otani et al. 2020; Liu, Qu, and Hu 2022; Yang et al. 2021) have shown that TSGV models are susceptible to dataset biases. They perform the grounding task through shortcuts created by dataset biases rather than the alignment between query texts and corresponding visual regions, resulting in poor generalization performance.

From the perspective of the dataset distribution, given samples that contain similar semantic components in the

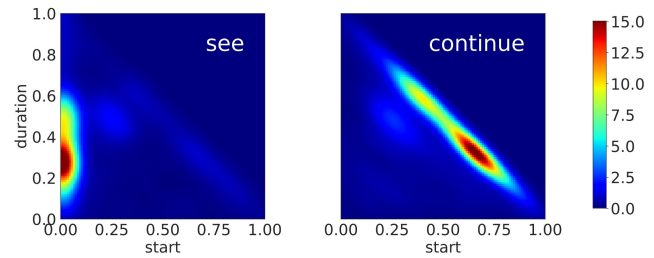


Figure 1: The spurious correlation between query words and temporal location of target moments. The horizontal and vertical axes represent the normalized starting time and duration of the target moment, respectively. The color represents the text-video pair density, which is obtained by using kernel density estimation with the Gaussian kernel.

input video or query text, the bias originates from the uneven temporal distribution of the corresponding target moments. As shown in Figure 1, in the widely used ActivityNet dataset, for samples containing the word “see” in the query text, their target moments tend to be concentrated in the first half of the video, and only a few target moments are located elsewhere in the video. This uneven distribution leads to unexpected spurious correlations between query words and target moments, which are easily captured by TSGV models. Once the query contains the word “see”, the model will predict the target moment as the first half of the video with a high probability. Similar phenomena also exist in the visual modality. Hence, generating samples to break these correlations and form a uniform temporal distribution of target moments is an effective debiasing strategy.

However, due to the rich semantic content in the video and text, we can not enumerate all the coupling relationships between the target moment and the semantic component of the video/text to generate corresponding samples. It is impossible to construct an ideal dataset without dataset biases. Therefore, Zhang et al. (Zhang et al. 2021c) modify the relative positions of target moments through video clipping to form a more uniform temporal distribution of target moments. Liu et al. (Liu, Qu, and Hu 2022) replace certain verbs or nouns in the query with similar vocabulary from the dataset to obtain negative samples for the coupling re-

*Corresponding author.

Copyright © 2024, Association for the Advancement of Artificial Intelligence (www.aaai.org). All rights reserved.

lationship between query words and target moments. These methods only disrupt a fixed quantity of dataset biases because of the limited diversity of words in the dataset and the limited relative positions of target moments.

Based on the above analysis, we propose the bias-conflict sample synthesis and adversarial removal debias strategy (BSSARD) for TSGV. Its core idea is that in the training stage, we randomly generate fake target moments for each real sample. Then we use the bias generator to generate visual or linguistic bias features condition on these fake target moments and construct bias-conflict samples that are falsely associated with the synthetic target moments. Through adversarial training, the bias discriminator should accurately judge that the bias-conflict sample contains biases and predict the original target moment. In essence, it will generate some samples for all the spurious correlations between the temporal position of the target moments and the visual/text modality data. It greatly destroys the uneven temporal distribution of the target moments in the TSGV datasets and disrupts language and visual biases simultaneously.

Specifically, BSSARD consists of two bias generators and a grounding model with a bias discriminator. Given a video-text pair (I_v, I_q) with target moment (y_s^r, y_e^r) , BSSARD will iteratively generate visual/text bias-conflict samples to form real and fake samples for adversarial debiasing. We first randomly generate a fake target moment (y_s^f, y_e^f) . Mimicking the spurious correlation between the visual feature and the fake target moment, we use the visual bias generator to produce a bias vector based on (y_s^f, y_e^f) , and add it to the visual feature of I_v , which constructs the bias-conflict sample (\tilde{I}_v, I_q) . Through (\tilde{I}_v, I_q) , the visual bias generator aims to force the grounding model to produce (y_s^f, y_e^f) and determine the input is a sample without bias. Instead, the grounding model needs to produce (y_s^r, y_e^r) for (I_v, I_q) and determine it is a sample without bias. Meanwhile, it should also produce (y_s^r, y_e^r) for (\tilde{I}_v, I_q) and determine it is a sample with bias. For the query bias generator, the process is similar. Through adversarial training, bias generators continuously introduce biases and generate bias-conflicting samples to deceive the grounding model. Meanwhile, the grounding model continuously eliminates the introduced biases, which requires it to model cross-modality alignment information to accomplish the grounding task. Hence, the final model can effectively resist the influence of dataset biases and achieve better generalization performance.

Experimental results on the repartitioned Charades-CD and ActivityNet-CD datasets demonstrate the effective debiasing capability of our approach.

Our main contributions are as follows:

- We propose a novel debiasing strategy, which generates bias-adversarial samples for most dataset biases and performs debias through adversarial training.
- We propose a debias network with two bias generators, a grounding block, and a bias discriminator, which can effectively eliminate visual and language biases.
- Extensive experiments on the OOD-test set demonstrate that BSSARD achieves great debias performance.

Related Work

Temporal Sentence Grounding in Video

TSGV methods are generally divided into proposal-based and proposal-free models. Proposal-based methods first generate a large number of candidate proposals, and then score all proposals with the language queries. Anchor-based proposal generation methods (Yu et al. 2021; Wang, Ma, and Jiang 2020; Qu et al. 2020; Zhang et al. 2019; Yuan et al. 2019) pre-define some boxes of specific proportions and directly generate proposals on the multi-modal features. 2D-based proposal generation methods (Zhang et al. 2020b, 2021d; Wang et al. 2021; Gao et al. 2021; Gao and Xu 2021; Hu et al. 2021) extend anchors to 2D to more finely model the positional relationships between proposals. Proposal-free methods are divided into regression-based and span-based methods. Regression-based methods (Yuan, Mei, and Zhu 2019; Lu et al. 2019; Zeng et al. 2020; Mun, Cho, and Han 2020; Ghosh et al. 2019; Zheng et al. 2023a; Wang et al. 2023) directly regress start and end timestamps. Such methods mainly focus on designing various feature encoding and cross-modal reasoning strategies to achieve precise localization. Span-based methods (Tang et al. 2021; Zhao et al. 2021; Zhang et al. 2021b,a, 2020a; Zheng et al. 2023b) directly predict the probability of each video segment as the start and end position of the target moment.

Model Debiasing

Solutions for mitigating dataset bias are divided into two categories: ensemble-based methods and additional constraint-based methods. Ensemble-based methods (Dagaev et al. 2021; Han et al. 2021; Liu, Qu, and Hu 2022) involve using weak models to learn the bias and then assessing the bias of samples based on the weak models. Biased samples are then given lower weights in the main model to achieve debias. Constraint-based methods (Hao et al. 2022a; Darlow, Jastrzębski, and Storkey 2020; Yang et al. 2021; Lan et al. 2023; Qi et al. 2023; Lan et al. 2022; Yoon et al. 2023) usually entail designing special structures and adding extra tasks to the model. This approach can separate bias from true rules, forcing the model to learn the true rules to complete the task. In contrast to the above methods, we propose to synthesize bias-conflict samples and disrupt the uneven distribution of the target moments for samples with similar semantic components, which forces models to learn useful alignment visual-language information for grounding.

Method

Overview

Our bias-conflict sample synthesis and adversarial removal debias strategy (BSSARD) is shown in Figure 2, which is based on a span-based grounding model and incorporates a Visual Bias Generator (VBG), a Query Bias Generator (QBG), and a Bias Discriminator (BD).

In the training stage, given a video-query pair (I_v, I_q) with the target moment (y_s^r, y_e^r) , we first utilize the visual and textual feature extractor to capture feature representations V and Q . On the one hand, we feed the original V

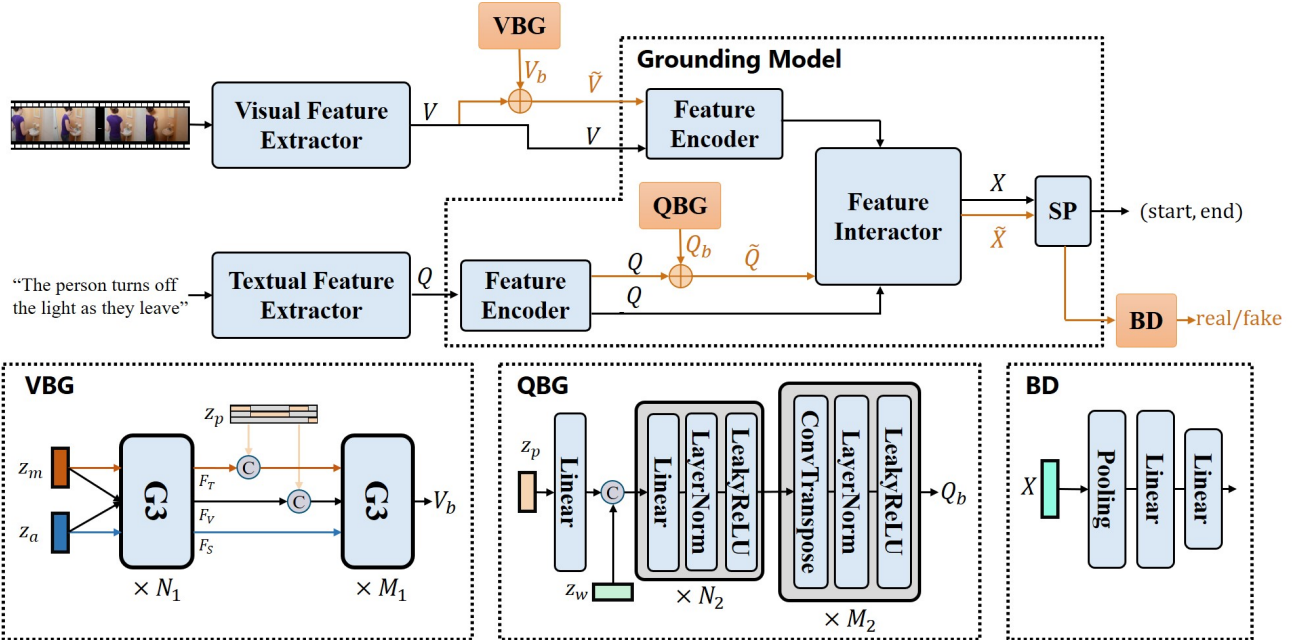


Figure 2: An overview of our BSSARD. The orange background is only used during the training period. Best viewed in color.

and Q into the feature encoder and feature interactor to obtain real sample feature X . Then, the span predictor (SP) should accurately produce the start and end time of the target moment. Meanwhile, the bias discriminator module should accurately predict it as the real sample. On the other hand, given a fake temporal location $z_p = (y_s^f, y_e^f)$ of the target moment obtained through random uniform sampling from the video frames, we employ VBG to generate visual bias feature V_b and element-wise add it to the real sample feature V , which produces \tilde{V} . Similar to the real sample, we obtain bias-conflict sample feature \tilde{X} . It has two labels, one is the temporal position (y_s^r, y_e^r) of the real target moment and the other is the fake temporal position (y_s^f, y_e^f) . The bias generator wants to generate shortcut features to trick SP into generating a target moment similar to z_p and trick BD into judging the current sample as the real sample. Instead, the SP will try to generate target moments as close as (y_s^r, y_e^r) and the BD will judge it as a sample with bias. Similarly, we also employ QBG to generate textual bias feature Q_b and perform the above process. The synthesized bias features simulate all kinds of spurious correlations between the semantic information of video/text and the temporal position of the target clips. Through adversarial training, it effectively mitigates visual and linguistic biases. In the inference stage, the VBG, QBG, and BD components are removed.

Bias Generator

The bias generator generates bias-conflict sample features based on synthesized spurious relationships between the unimodality information and the temporal positional labels.

Visual Bias Generator We construct VBG by the G^3 module (Wang et al. 2020), which encodes video features by

decoupling appearance and motion content. The VBG contains three randomly generated variables z_a , z_m , and z_p as inputs, and generates visual bias vector V_b for constructing bias-conflict samples. These random variables guarantee the diversity and randomness of the bias generator.

Especially, the z_a and z_m are random vectors that follow a normal distribution and represent appearance and motion content, respectively. VBG first inputs z_a and z_m into N_1 stacked G^3 , and produces three visual stream features, named temporal stream F_T , spatial stream F_S and video stream F_V . Then, we randomly generate a fake temporal label $z_p \in \mathbb{R}^{3 \times n}$ of the target clip, which is obtained through random uniform sampling from the video frame sequence within the range of $[0, n - 1]$. Its three dimensions are mutually exclusive and represent whether the segment contains background, foreground, or ignored data. It provides the temporal position conditional information that the bias generator requires. Subsequently, z_p is concatenated with F_T and F_V to introduce temporal position information. Next, VBG outputs the visual bias vector $V_b \in \mathbb{R}^{n \times d}$ through M_1 stacked G^3 . Finally, we add V_b to V and obtain visual bias conflict sample feature \tilde{V} ,

$$V_b = VBG(z_a, z_m, z_p) \quad (1)$$

$$\tilde{V} = V_b + V$$

where n and d are the video length and feature dimension.

Query Bias Generator We construct QBG by a simple fully connected structure and transpose convolutional structure. The QBG needs two randomly generated variables z_w and z_p as inputs and generates textual bias vector Q_b for constructing bias-conflict samples.

Specifically, we randomly sample z_p from a normal distribution, which is a random vector of length n and represents

the synthetic label of the fake target video moment. Then we embed it using a fully connected layer, which provides the temporal position information for the feature generation. To enhance randomness and diversity, QBG also generates a random vector z_w from a normal distribution to introduce the context for the feature generation, which is concatenated with the encoded position feature. We use N_2 linear layers and M_2 transposed convolution layers to produce the word sequence bias feature $Q_b \in \mathbb{R}^{m \times d}$. Finally, we add Q_b to Q and obtain query bias conflict sample feature \tilde{Q} ,

$$\begin{aligned} Q_b &= QBG(z_w, z_p) \\ \tilde{Q} &= Q_b + Q \end{aligned} \quad (2)$$

where m represents the length of the query text.

Grounding Model

The grounding model consists of a feature encoder, feature interactor, span predictor (SP), and bias discriminator (BD). BD is a binary classifier that identifies whether the sample contains biases. SP should make correct temporal grounding predictions for both regular and bias-conflict samples.

For the normal samples without synthetic bias features, V and Q are encoded by the feature encoder and feature interactors to generate cross-modal representations X . Subsequently, the SP and BD make predictions,

$$\begin{aligned} p_s^r, p_e^r &= SP(X) \in \mathbb{R}^n, \mathbb{R}^n \\ p_d^r &= BD(X) \in \mathbb{R}^2 \end{aligned} \quad (3)$$

where p_s^r and p_e^r represent the predicted start and end positions of the target moment for the real sample, and p_d^r represents the probability of the sample containing bias.

For bias-conflict samples, we iteratively encode \tilde{V} and Q or V and \tilde{Q} in each training iteration by the feature encoder and feature interactor to generate cross-modal representation \tilde{X} . Subsequently, the SP and BD make predictions,

$$\begin{aligned} p_s^f, p_e^f &= SP(\tilde{X}) \in \mathbb{R}^n, \mathbb{R}^n \\ p_d^f &= BD(\tilde{X}) \in \mathbb{R}^2 \end{aligned} \quad (4)$$

where p_s^f and p_e^f represent the predicted start and end positions of the target moment for the bias-conflict sample, and p_d^f represents the probability of the sample containing bias.

Training Objectives

Training Process As shown in Algorithm 1, we train the two bias generators alternately in each training step. We detail the bias generator loss L^g and the discriminator loss L^d .

Bias Generator Training Objectives The visual/query bias generator aims to deceive the bias discriminator and induce the span predictor to produce the given fake labels.

We use cross-entropy loss to trick the bias discriminator,

$$L_{cls}^g = f_{CE}(p_d^r, 0) \quad (5)$$

where p_d^r represents the predicted sample flag. 0 indicates the current sample is a real sample without synthetic bias.

Algorithm 1: Training process in one epoch.

Require: VBG; QBG; GD;
Ensure: TSGV model

- 1: **for** each training iteration **do**
- 2: Sample $(V, Q), (y_s^r, y_e^r)$
- 3: Sample $z_m, z_a, z_p, (y_s^f, y_e^f)$
- 4: $V_b \leftarrow \text{VBG}(z_m, z_a, z_p)$
- 5: $\tilde{V} \leftarrow V + V_b, \tilde{Q} \leftarrow Q$
- 6: Get $p_s^r, p_e^r, p_d^r, p_s^f, p_e^f, p_d^f$ by Equation 3 and 4
- 7: Calculate L^g and train VBG, freeze GD
- 8: Calculate L^d and train GD, freeze VBG
- 9: Sample $z_w, z_p, (y_s^f, y_e^f)$
- 10: $Q_b \leftarrow \text{QBG}(z_w, z_p)$
- 11: $\tilde{V} \leftarrow V, \tilde{Q} \leftarrow Q + Q_b$
- 12: Get $p_s^r, p_e^r, p_d^r, p_s^f, p_e^f, p_d^f$ by Equation 3 and 4
- 13: Calculate L^g and train QBG, freeze GD
- 14: Calculate L^d and train GD, freeze QBG
- 15: **end for**

It encourages the generator to generate samples that the BD will classify as unbiased.

To induce span predictor, we use cross-entropy loss:

$$L_{loc}^g = \frac{1}{2} [f_{CE}(p_s^f, y_s^f) + f_{CE}(p_e^f, y_e^f)] \quad (6)$$

This encourages the bias generator to generate bias-conflict samples that can deceive the grounding model.

The total training loss of the bias generator is

$$L^g = L_{loc}^g + \lambda_1 L_{cls}^g \quad (7)$$

where λ_1 is a weight hyperparameter.

Discriminator Training Objectives The discriminator needs to distinguish between real and bias-conflict samples and predict the true target moments.

For the bias discriminator, we use cross-entropy loss,

$$L_{cls}^d = f_{CE}(p_d^r, 0) + f_{CE}(p_d^f, 1) \quad (8)$$

It encourages the discriminator to accurately judge real and synthetic samples.

For the temporal grounding, we use the traditional span-based cross-entropy loss,

$$\begin{aligned} L_{loc}^d &= \frac{1}{2} [f_{CE}(p_s^r, y_s^r) + f_{CE}(p_e^r, y_e^r)] \\ &+ \frac{1}{2} [f_{CE}(p_s^f, y_s^r) + f_{CE}(p_e^f, y_e^r)] \end{aligned} \quad (9)$$

Besides, we find it advantageous to incorporate a sample-based distance metric such as KL divergence. Consequently, we introduce an additional objective,

$$L_{kl}^d = D_{kl}(p_s^r \| p_s^f) + D_{kl}(p_e^r \| p_e^f) \quad (10)$$

Here, Equation 9 aligns the predictions towards the real labels, and Equation 10 limits the predictions of bias-conflict samples to not deviate much from the predictions of the corresponding original samples. Meanwhile, KL divergence is

Method	Charades-CD						ActivityNet-CD					
	OOD			IID			OOD			IID		
	r1i5	r1i7	mIoU	r1i5	r1i7	mIoU	r1i5	r1i7	mIoU	r1i5	r1i7	mIoU
2D-TAN (Zhang et al. 2020b)	28.18	13.73	34.22	46.48	28.76	42.73	18.86	9.77	28.31	40.87	28.95	44.99
LG (Mun, Cho, and Han 2020)	42.90	19.29	39.43	51.28	28.68	45.16	23.85	10.96	28.46	46.41	29.28	44.62
DRN (Zeng et al. 2020)	31.11	15.17	23.05	42.04	23.32	28.21	-	-	-	-	-	-
VSLNet (Zhang et al. 2020a)	34.10	17.87	36.34	43.26	28.43	42.92	20.03	10.29	28.18	47.81	29.07	46.33
DCM (Yang et al. 2021)	40.51	21.02	40.99	52.50	35.28	48.74	20.86	11.07	28.08	42.15	29.69	45.20
SVTG (Hao et al. 2022a)	46.67	27.08	44.30	57.59	37.79	50.93	24.57	13.21	30.45	48.07	32.15	47.03
MDD (Lan et al. 2022)	40.39	22.70	-	52.78	34.71	-	20.80	11.66	-	43.63	31.44	-
QAVE (Hao et al. 2022b)	37.84	19.67	38.45	47.63	29.28	44.17	21.39	10.86	28.41	44.58	27.42	44.28
BSSARD-QAVE	44.47	26.16	42.95	54.31	37.67	49.41	23.11	12.17	29.40	46.04	30.06	45.56
EXCL (Ghosh et al. 2019)	39.61	19.35	38.81	47.18	26.59	44.02	23.38	12.66	29.19	45.76	29.62	46.42
BSSARD-EXCL	41.93	22.53	40.9	50.00	31.86	46.47	23.75	12.93	29.26	46.98	30.34	46.12
VSLNet* (Zhang et al. 2020a)	43.08	22.52	41.52	52.86	34.87	48.23	25.40	13.51	30.33	48.07	31.19	46.94
BSSARD-VSLNet*	47.20	27.17	44.59	55.65	36.33	50.45	27.02	14.93	31.49	49.67	33.72	48.54

Table 1: Comparison results with state-of-the-arts. VSLNet* replaces the encoder in VSLNet with a transformer block.

a regularization method to prevent the generator from overfitting training data and improve the generalization ability.

The total training loss of the discriminator is:

$$L^d = L_{loc}^d + \lambda_2 L_{cls}^d + \lambda_3 L_{kl}^d \quad (11)$$

where λ_2 and λ_3 are weight hyperparameters.

Experiment

Experiment Setup

Datasets We conduct experiments on the repartitioned Charades-CD and ActivityNet-CD (Lan et al. 2022). In these repartitioned datasets, the target moments of samples in the training, val, and test-iid sets are independent and identically distributed, while the test-ood set contains out-of-distribution samples. We can verify the debias ability of different models according to the grounding performance on the test-ood set and the performance difference between test-iid and test-ood sets.

Metrics We use evaluation metrics of $R@n$, $\text{IoU}=m$, and mIoU . $R@n$, $\text{IoU}=m$ measures the proportion of test samples in which at least one of the top- n localization results has an IoU score greater than m . The mIoU measures the average IoU score across all test samples. We set n to 1 and m to either 0.5 or 0.7, and use r1i5 and r1i7 to denote $R@1$, $\text{IoU}=0.5$ and $R@1$, $\text{IoU}=0.7$, respectively.

Implementation Details For the text feature extractor, we use 300d GloVe (Pennington, Socher, and Manning 2014) vectors for initialization. For the visual feature extractor, we use pre-trained I3D (Carreira and Zisserman 2017) and C3D (Tran et al. 2015) features. For the visual bias generator, we set N_1 to 4 and M_1 to 2. For the query bias generator, we set N_2 to 2 and M_2 to 4. During the training process, we use the AdamW (Loshchilov and Hutter 2017) optimizer, with a batch size of 16, and an initial learning rate of 0.001. We set λ_1 to 1, λ_2 to 1, and λ_3 to 1.

Row	BG			Grounding			OOD		
	L_{loc}^g	L_{cls}^g	L_{loc}^d	L_{cls}^d	L_{kl}^d	r1i5	r1i7	mIoU	
1	-	-	✓	-	-	43.08	22.52	41.52	
2	✓	-	✓	-	-	46.64	26.40	43.49	
3	✓	-	✓	-	✓	45.99	26.16	44.02	
4	-	✓	✓	✓	✓	45.16	25.72	43.18	
5	-	✓	✓	✓	✓	46.22	26.40	44.22	
6	✓	✓	✓	✓	-	47.41	26.84	44.00	
7	✓	✓	✓	✓	✓	47.20	27.17	44.59	

Table 2: Ablation study about loss functions.

Comparison with State-of-the-Arts

To verify the universality of our debias strategy, we implement our BSSARD on multiple existing backbones QAVE, ExCL, and VSLNet*. The experiment results on Charades-CD and ActivityNet-CD datasets are presented in Table ???. We can see that our approach can significantly improve the grounding performance of different backbones on most evaluation metrics for OOD and IID test sets in both datasets. This indicates that our method has stronger debias and grounding ability. Besides, although our method shows the best performance in ActivityNet-CD’s IID (BSSARD-VSLNet*), it works weaker than SVTG in Charades-CD’s IID test set. This is due to the IID test set of Charades-CD containing a higher proportion of biased samples.

Ablation Study

We conduct abundant ablation studies on Charades-CD datasets over BSSARD-VSLNet* backbones.

Loss Terms We analyze the impact of each loss function and their combinations on the grounding performance. Table ?? summarizes the results. We can see that each loss function has its validity, and the combination of generation

Method	OOD			IID		
	r1i5	r1i7	mIoU	r1i5	r1i7	mIoU
QAVE	37.84	19.67	38.45	47.63	29.28	44.17
QAVE-Q	41.96	23.20	40.97	50.18	32.56	47.11
QAVE-V	42.79	22.34	41.03	54.07	33.41	48.31
BSSARD-QAVE	44.47	26.16	42.95	54.31	37.67	49.41
ExCL	39.61	19.35	38.81	47.18	26.59	44.02
ExCL-Q	39.94	19.7	39.05	48.90	26.59	44.72
ExCL-V	39.10	19.21	38.77	47.79	30.76	45.58
BSSARD-ExCL	41.93	22.53	40.9	50.00	31.86	46.47
VSLNet*	43.08	22.52	41.52	52.86	34.87	48.23
VSLNet*-Q	44.86	25.30	42.91	53.10	33.78	49.13
VSLNet*-V	45.16	25.48	44.04	55.89	36.57	51.60
BSSARD-VSLNet*	47.20	27.17	44.59	55.65	36.33	50.45

Table 3: Ablation study about bias generator.

visual	language	r1i5	r1i7	mIoU
before	before	47.32	26.46	44.30
before	after	47.20	27.17	44.59
after	before	45.45	25.30	42.66
after	after	46.67	25.90	43.69

Table 4: Ablation study about bias injection positions. “before” and “after” represent the injection position before and after the feature encoder, respectively.

and adversarial losses can further improve the grounding performance on the OOD test set. Besides, the L_{kl}^d leads to performance improvements in most cases. However, the improvement is limited when L_{cls}^d is not used. This is because L_{kl}^d depends on the grounding model’s attention to the bias features brought by L_{cls}^d .

Bias Generator We analyze the impact of visual and query bias generators on different backbones and show the results in Tables ?? . *-V and *-Q refer to the backbone model that uses only visual and query bias generators, respectively. The results show that the visual and query bias generators are effective on all backbones, and the two generators complement each other. Besides, we find that the performance of VSLNet*-V is even better than BSSARD-VSLNet* on the IID test set. This is mainly due to two reasons, one is that the powerful cross-modality alignment ability of VSLNet* weakens the integration effect of the two bias generators, and the other is the presence of numerous language bias samples in the IID test set.

Bias Injection Positions We explore the effect of bias feature injection positions. The injection position determines which features the bias generator needs to generate bias on and which parts of the grounding model need to complete debias task. For visual and language biases, we separately test the injection position before and after the feature encoder. The results are shown in Table ?? . We can see that injecting the visual bias feature before the visual feature en-

z_p	concat	r1i5	r1i7	mIoU
\mathbb{R}^n	F_T, F_V	46.40	26.40	44.07
$\mathbb{R}^{3 \times n}$	F_T, F_V	47.20	27.17	44.59
$\mathbb{R}^{3 \times n}$	F_T, F_V, F_S	46.70	26.28	44.15

Table 5: Ablation study about fusion method of z_p .

Training strategy	r1i5	r1i7	mIoU
alternate each epoch	46.79	26.76	44.53
random each step	45.81	25.84	43.81
alternate each step	47.20	27.17	44.59

Table 6: Ablation study about training strategy.

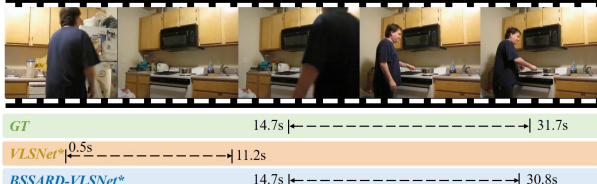
coder and injecting the language bias feature after the language feature encoder is the most effective. This primarily depends on the distinct characteristics of vision and text data and the need for both accuracy and diversity in generated bias features. First, the intricate nature of video content and the high-dimensional visual feature space pose serious challenges for the feature encoder that aims to map visual and textual features into a shared space for multi-modal feature alignment. Injecting visual bias before the feature encoder reduces the encoder’s learning complexity, enabling the model to differentiate real from synthesized visual features. Second, introducing language bias after the feature encoder helps the model better capture bias during the multi-modal feature alignment stage. Third, multiple injection positions increase the diversity of generated bias features.

Besides, we inject bias in the feature domain instead of the input data because it is more controllable to generate high-quality sample features. If we directly generate video samples, the generator should not only capture the bias information but also learn the original video representation, which greatly increases the learning difficulty.

Fusion Method of z_p in VBG We investigate the impact of different fusion methods between z_p and visual features in VBG. Table ?? summarizes the results on the OOD test set. We test three fusion methods, (1) encoding the temporal position as $z_p \in \mathbb{R}^n$ and fusing it with the temporal stream F_T and video stream F_V . (2) encoding the temporal position as $z_p \in \mathbb{R}^{3 \times n}$ and fusing it with F_T and F_V . (3) encoding the temporal position as $z_p \in \mathbb{R}^{3 \times n}$ and fusing it with the F_T , F_V and spatial stream F_S . The results demonstrate that the second method is the most effective. This is because $z_p \in \mathbb{R}^{3 \times n}$ can better represent temporal position information, and only the time stream F_T and video stream F_V containing temporal information that can better utilize temporal position information.

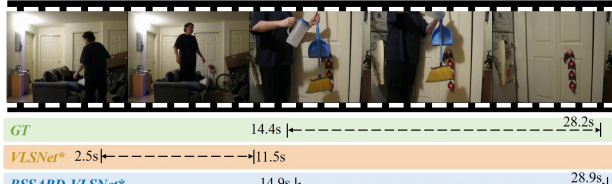
Training Strategy for Bias Generators We investigate the impact of the training order of two bias generators and show results in Table ?? . We test three training strategies: (1) alternately training the two bias generators at each epoch. (2) randomly selecting one bias generator for training at each training step. (3) alternately training the two bias genera-

Query: person **cooking** something on the stove.



(a) “cook” suggests the target moment starts at the video start.

Query: person **holds** up a broom.



(c) “hold” suggests the target moment starts at the video start.

Query: person they **start** sneezing.



(b) “start” implies the target moment is at the end of the video.

Query: person **eating** it.



(d) “hold” suggests the target moment starts at the video start.

Figure 3: The visualization comparison results between VLSNet* and BSSARD-VLSNet*.

Setting	B-VSLNet	VSLNet	B-QAVE	QAVE
Original query	47.20	43.08	44.47	37.84
Random query	15.11	18.31	29.87	31.17
Gap	67.99% ↓	57.50% ↓	32.83% ↓	17.63% ↓

Table 7: Comparison results under random text input.

tors at each training step. The experimental results indicate that the third training strategy is optimal. This is mainly because alternate training the two bias generators can avoid the model overfitting into a certain debias approach.

Analysis of the Debias Effect

The Verification of Mitigating Bias We randomly shuffle the words in each query text, which disrupts potential spurious correlations among query text and target moments. It also prevents the model from relying on visual-language alignment unless it depends on visual bias. Table ?? shows BSSARD achieves more significant performance degradation. This indicates our approach relies less on bias correlations beyond query text to perform grounding.

Qualitative Analysis We also compare the debias effect of our BSSARD-VLSNet* and VLSNet* at the sample level in Figure 3. First, we give the temporal distribution of the target moment for samples with common verbs in the Charades-CD training set in Figure 4. This indicates each verb contains prior knowledge for the localization of the target video clip. For example, the verb “cook” indicates that the temporal location of the target moments for most samples is the first half of the video. Hence, if the query text contains “cook” and the model will output the target moment with high probability in the first half of the video, which is the phenomenon of VLSNet* shown in Figure 3(a). However, the result of our

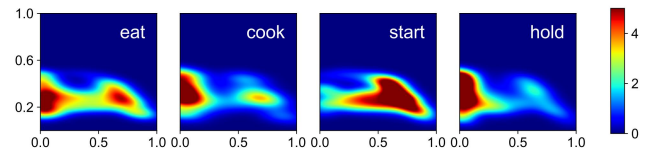


Figure 4: The temporal distribution of target moments for video-text samples with certain common verbs. The horizontal and vertical axes denote the normalized starting time and duration of the target moment, respectively. The color represents the sample density.

BSSARD-VLSNet* is not affected by the bias in the training set. The other three examples also show that the VLSNet* model relies on the bias in the training set for prediction, while our BSSARD-VLSNet* can effectively reduce the dependence on the bias and shift the model’s attention back to cross-modality matching to make correct predictions.

Conclusion

In this paper, we propose a novel adversarial training debias framework for TSGV task. It dynamically generates bias-conflict samples by exploiting all kinds of spurious relationships between single-modality features and the target moments, which can effectively remove the bias dependency of the TSGV models. In essence, the debias is achieved through directional data augmentation, which breaks the uneven temporal distribution of the target moments for samples that contain similar semantic components. Extensive experiments on Charades-CD and ActivityNet-CD datasets demonstrate the effectiveness of our strategy. In the future, we will apply our method to a wider range of scenarios, such as debias in visual question-answering task, and also eliminate cross-modality combination bias problems.

Acknowledgments

This work was supported in part by the National Natural Science Foundation of China under Grant U21B2038, 62306092, 61976069, 62022083, and 62236008.

References

Carreira, J.; and Zisserman, A. 2017. Quo vadis, action recognition? a new model and the kinetics dataset. In *proceedings of the IEEE Conference on Computer Vision and Pattern Recognition*, 6299–6308.

Dagaev, N.; Roads, B. D.; Luo, X.; Barry, D. N.; Patil, K. R.; and Love, B. C. 2021. A too-good-to-be-true prior to reduce shortcut reliance. *arXiv preprint arXiv:2102.06406*.

Darlow, L.; Jastrzębski, S.; and Storkey, A. 2020. Latent adversarial debiasing: Mitigating collider bias in deep neural networks. *arXiv preprint arXiv:2011.11486*.

Gao, J.; Sun, X.; Xu, M.; Zhou, X.; and Ghanem, B. 2021. Relation-aware video reading comprehension for temporal language grounding. *arXiv preprint arXiv:2110.05717*.

Gao, J.; and Xu, C. 2021. Fast video moment retrieval. In *Proceedings of the IEEE/CVF International Conference on Computer Vision*, 1523–1532.

Ghosh, S.; Agarwal, A.; Parekh, Z.; and Hauptmann, A. 2019. Excl: Extractive clip localization using natural language descriptions. *arXiv preprint arXiv:1904.02755*.

Han, X.; Wang, S.; Su, C.; Huang, Q.; and Tian, Q. 2021. Greedy gradient ensemble for robust visual question answering. In *Proceedings of the IEEE/CVF International Conference on Computer Vision*, 1584–1593.

Hao, J.; Sun, H.; Ren, P.; Wang, J.; Qi, Q.; and Liao, J. 2022a. Can Shuffling Video Benefit Temporal Bias Problem: A Novel Training Framework for Temporal Grounding. In *Proceedings of the European Conference on Computer Vision*, 130–147.

Hao, J.; Sun, H.; Ren, P.; Wang, J.; Qi, Q.; and Liao, J. 2022b. Query-aware video encoder for video moment retrieval. *Neurocomputing*, 483: 72–86.

Hu, Y.; Nie, L.; Liu, M.; Wang, K.; Wang, Y.; and Hua, X.-S. 2021. Coarse-to-fine semantic alignment for cross-modal moment localization. *IEEE Transactions on Image Processing*, 30: 5933–5943.

Lan, X.; Yuan, Y.; Chen, H.; Wang, X.; Jie, Z.; Ma, L.; Wang, Z.; and Zhu, W. 2023. Curriculum multi-negative augmentation for debiased video grounding. In *Proceedings of the AAAI Conference on Artificial Intelligence*.

Lan, X.; Yuan, Y.; Wang, X.; Chen, L.; Wang, Z.; Ma, L.; and Zhu, W. 2022. A closer look at debiased temporal sentence grounding in videos: Dataset, metric, and approach. *ACM Transactions on Multimedia Computing, Communications, and Applications*.

Liu, D.; Qu, X.; and Hu, W. 2022. Reducing the vision and language bias for temporal sentence grounding. In *Proceedings of the 30th ACM International Conference on Multimedia*, 4092–4101.

Loshchilov, I.; and Hutter, F. 2017. Fixing weight decay regularization in adam.

Lu, C.; Chen, L.; Tan, C.; Li, X.; and Xiao, J. 2019. Debug: A dense bottom-up grounding approach for natural language video localization. In *Proceedings of the Conference on Empirical Methods in Natural Language Processing and the 9th International Joint Conference on Natural Language Processing*, 5144–5153.

Mun, J.; Cho, M.; and Han, B. 2020. Local-global video-text interactions for temporal grounding. In *Proceedings of the IEEE/CVF Conference on Computer Vision and Pattern Recognition*, 10810–10819.

Otani, M.; Nakashima, Y.; Rahtu, E.; and Heikkilä, J. 2020. Uncovering hidden challenges in query-based video moment retrieval. *arXiv preprint arXiv:2009.00325*.

Pennington, J.; Socher, R.; and Manning, C. D. 2014. Glove: Global vectors for word representation. In *Proceedings of the conference on empirical methods in natural language processing*, 1532–1543.

Qi, Z.; Wang, S.; Su, C.; Su, L.; Huang, Q.; and Tian, Q. 2023. Self-Regulated Learning for Egocentric Video Activity Anticipation. *IEEE Transactions on Pattern Analysis and Machine Intelligence*, 45(6): 6715–6730.

Qu, X.; Tang, P.; Zou, Z.; Cheng, Y.; Dong, J.; Zhou, P.; and Xu, Z. 2020. Fine-grained iterative attention network for temporal language localization in videos. In *Proceedings of the 28th ACM International Conference on Multimedia*, 4280–4288.

Tang, H.; Zhu, J.; Liu, M.; Gao, Z.; and Cheng, Z. 2021. Frame-wise cross-modal matching for video moment retrieval. *IEEE Transactions on Multimedia*, 24: 1338–1349.

Tran, D.; Bourdev, L.; Fergus, R.; Torresani, L.; and Paluri, M. 2015. Learning spatiotemporal features with 3d convolutional networks. In *Proceedings of the IEEE international conference on computer vision*, 4489–4497.

Wang, H.; Zha, Z.-J.; Li, L.; Liu, D.; and Luo, J. 2021. Structured multi-level interaction network for video moment localization via language query. In *Proceedings of the IEEE/CVF Conference on Computer Vision and Pattern Recognition*, 7026–7035.

Wang, J.; Ma, L.; and Jiang, W. 2020. Temporally grounding language queries in videos by contextual boundary-aware prediction. In *Proceedings of the AAAI Conference on Artificial Intelligence*, volume 34, 12168–12175. ISBN 2374-3468.

Wang, Y.; Bilinski, P.; Bremond, F.; and Dantcheva, A. 2020. G3AN: Disentangling appearance and motion for video generation. In *Proceedings of the IEEE/CVF Conference on Computer Vision and Pattern Recognition*, 5264–5273.

Wang, Z.; Zhao, Y.; Huang, H.; Xia, Y.; and Zhao, Z. 2023. Scene-robust Natural Language Video Localization via Learning Domain-invariant Representations. In *Findings of the Association for Computational Linguistics: ACL 2023*, 144–160.

Yang, X.; Feng, F.; Ji, W.; Wang, M.; and Chua, T.-S. 2021. Deconfounded video moment retrieval with causal intervention. In *Proceedings of the 44th International ACM SIGIR Conference on Research and Development in Information Retrieval*, 1–10.

Yoon, S.; Hong, J. W.; Eom, S.; Yoon, H. S.; Yoon, E.; Kim, D.; Kim, J.; Kim, C.; and Yoo, C. D. 2023. Counterfactual Two-Stage Debiasing For Video Corpus Moment Retrieval. In *ICASSP 2023-2023 IEEE International Conference on Acoustics, Speech and Signal Processing*, 1–5. IEEE.

Yu, X.; Malmir, M.; He, X.; Chen, J.; Wang, T.; Wu, Y.; Liu, Y.; and Liu, Y. 2021. Cross interaction network for natural language guided video moment retrieval. In *Proceedings of the 44th International ACM SIGIR Conference on Research and Development in Information Retrieval*, 1860–1864.

Yuan, Y.; Ma, L.; Wang, J.; Liu, W.; and Zhu, W. 2019. Semantic conditioned dynamic modulation for temporal sentence grounding in videos. *Advances in Neural Information Processing Systems*, 32.

Yuan, Y.; Mei, T.; and Zhu, W. 2019. To find where you talk: Temporal sentence localization in video with attention based location regression. In *Proceedings of the AAAI Conference on Artificial Intelligence*, volume 33, 9159–9166. ISBN 2374-3468.

Zeng, R.; Xu, H.; Huang, W.; Chen, P.; Tan, M.; and Gan, C. 2020. Dense regression network for video grounding. In *Proceedings of the IEEE/CVF Conference on Computer Vision and Pattern Recognition*, 10287–10296.

Zhang, H.; Sun, A.; Jing, W.; Zhen, L.; Zhou, J. T.; and Goh, R. S. M. 2021a. Natural language video localization: A revisit in span-based question answering framework. *IEEE transactions on pattern analysis and machine intelligence*.

Zhang, H.; Sun, A.; Jing, W.; Zhen, L.; Zhou, J. T.; and Goh, R. S. M. 2021b. Parallel attention network with sequence matching for video grounding. *arXiv preprint arXiv:2105.08481*.

Zhang, H.; Sun, A.; Jing, W.; and Zhou, J. T. 2020a. Span-based localizing network for natural language video localization. *arXiv preprint arXiv:2004.13931*.

Zhang, H.; Sun, A.; Jing, W.; and Zhou, J. T. 2021c. Towards debiasing temporal sentence grounding in video. *arXiv preprint arXiv:2111.04321*.

Zhang, M.; Yang, Y.; Chen, X.; Ji, Y.; Xu, X.; Li, J.; and Shen, H. T. 2021d. Multi-stage aggregated transformer network for temporal language localization in videos. In *Proceedings of the IEEE/CVF Conference on Computer Vision and Pattern Recognition*, 12669–12678.

Zhang, S.; Peng, H.; Fu, J.; and Luo, J. 2020b. Learning 2d temporal adjacent networks for moment localization with natural language. In *Proceedings of the AAAI Conference on Artificial Intelligence*, volume 34, 12870–12877. ISBN 2374-3468.

Zhang, Z.; Lin, Z.; Zhao, Z.; and Xiao, Z. 2019. Cross-modal interaction networks for query-based moment retrieval in videos. In *Proceedings of the 42nd International ACM SIGIR Conference on Research and Development in Information Retrieval*, 655–664.

Zhao, Y.; Zhao, Z.; Zhang, Z.; and Lin, Z. 2021. Cascaded prediction network via segment tree for temporal video grounding. In *Proceedings of the IEEE/CVF Conference on Computer Vision and Pattern Recognition*, 4197–4206.

Zheng, M.; Gong, S.; Jin, H.; Peng, Y.; and Liu, Y. 2023a. Generating Structured Pseudo Labels for Noise-resistant Zero-shot Video Sentence Localization. In *Proceedings of the 61st Annual Meeting of the Association for Computational Linguistics*, 14197–14209.

Zheng, M.; Li, S.; Chen, Q.; Peng, Y.; and Liu, Y. 2023b. Phrase-level Temporal Relationship Mining for Temporal Sentence Localization. In *Proceedings of the AAAI Conference on Artificial Intelligence*.